Chemical Physics 406 (2012) 72–77

Contents lists available at SciVerse ScienceDirect

Chemical Physics

journal homepage: www.elsevier.com/locate/chemphys

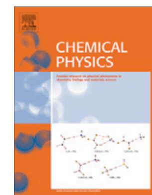

# Hydrophilic-like wettability of Cl-passivated Ge(001) surface

J.K. Bal [a,*], Sarathi Kundu [b], S. Hazra [a]

[a] Surface Physics Division, Saha Institute of Nuclear Physics, 1/AF Bidhannagar, Kolkata 700064, India
[b] Physical Sciences Division, Institute of Advanced Study in Science and Technology, Vigyan Path, Paschim Boragaon, Garchuk, Guwahati 781035, Assam, India

ARTICLE INFO

*Article history:*
Available online 16 August 2012

*Keywords:*
Surface passivation
Hydrophilic and hydrophobic surface
Langmuir–Blodgett film
X-ray reflectivity
Atomic force microscopy

ABSTRACT

The hydrophilic/hydrophobic nature of the Cl-passivated Ge(001) surface is investigated directly by contact angle (CA) measurement and indirectly by growing nickel arachidate Langmuir–Blodgett (LB) films on the Cl-passivated Ge(001) surface. Passivation of Ge(001) surface by Cl atoms is confirmed by X-ray photoelectron spectroscopy measurement. CA measurements show that the Cl-passivated Ge(001) surface has intermediate wettability, i.e., the surface has intermediate hydrophilic/hydrophobic behavior. Structural information obtained from the deposited LB films by using X-ray reflectivity and atomic force microscopy analysis shows that the surface is homogeneous and hydrophilic (∼85%), although very few effectively hydrophobic (∼15%) regions are present. Structural study in molecular level thus helps to identify the surface nature in nanometer level, which is not possible by simple macroscopic CA measurement. Specific electrostatic and dispersive effects of Cl atoms are possibly responsible for such hydrophilic-like nature of the Cl-passivated Ge(001) surface.

© 2012 Elsevier B.V. All rights reserved.

## 1. Introduction

Ge is considered as a promising material for the next generation microelectronic circuits, device fabrication [1–4], etc. due to its favorable electronic properties (e.g., narrower band gap, high electron and hole mobilities) compared with Si. The main difficulty for the application of Ge is to obtain a stable and defect free oxide ($GeO_x$) layer on Ge surface, as thermally grown $GeO_2$ shows poor dielectric properties such as water-soluble character. A stable and large defect free $GeO_x$/Ge interface unlike $SiO_x$/Si cannot be obtained. Hence, the elimination of surface oxide from Ge, before film deposition would be important for the utilization of Ge as device materials. In order to do that, chemical functionalization of Ge surface is essential. Passivation by wet chemical method is the best way to restore a surface contamination-free in the ambient conditions [5–10]. Although cleaning and passivation of Si surface have been extensively studied [11–16], but little attention is paid for Ge [5–17]. The well-established methods for cleaning Si cannot be directly applied to Ge because the oxide offers no protection in the latter case. There are different wet chemical passivations, namely, H- [14,15], Br- [16,17], Cl- [17–19], I-passivation [20], etc. Among these, Cl-passivation of Ge surfaces is drawing particular attention, because of the Ge–Cl bond strength and stability. In Cl-passivation, coverage of Cl atom can be achieved larger compared to H in the H-passivation of Ge surface [21]. On the other hand, Cl-passivation of Ge surface can be done very easily in wet chemical method by using only HCl in comparison with the chlorination of Si surface, since $GeO_2$ is soluble but $SiO_2$ is inert in HCl. However, for practical applications, a film has to be deposited on such passivated surface. The structure of the deposited films, typically LB films, strongly depends upon the hydrophilic or hydrophobic nature of the Cl-passivated Ge surface.

It is well accepted that the wetting/nonwetting i.e., hydrophilic/hydrophobic nature of a surface is easily identified by CA measurement [22,23], which is quite useful if the surface is homogeneous in macroscopic dimensions. However, if the surface is inhomogeneous i.e., if both hydrophobic and hydrophilic domains coexist and if the domain or spot size is of the order of few nanometer then through conventional CA measurements, it is not appropriate to estimate the overall nature of the substrate surface and not possible to investigate the nature of the individual spots. Such limitation of CA measurement can be overcome by depositing suitable LB films and determining its structures [24,25]. This is obviously an indirect method but very useful to obtain the nature of the surface domains in nanometer level. Thus, by studying the LB film structure one can predict about the homogeneity or inhomogeneity of the surface in nanodimension. From our previous study [24,25], the nature of the substrate surface was determined in the molecular level by depositing nickel arachidate (NiA) LB films. Moreover, there are some controversies regarding the nature of the Cl-passivated Si surface [18,19] and as the electronegativity of Si (∼1.9) and Ge (∼2.0) is nearly same then such type of controversies may arise in case of the Cl-passivated Ge surface also which needs a clear understanding. The structural information of the deposited LB

* Corresponding author. Present address: Laboratoire de Physique de l'Etat Condensé, UMR 6087 CNRS, Université du Maine, 72085 Le Mans, Cedex 9, France.
*E-mail address:* jayanta.bal@gmail.com (J.K. Bal).

0301-0104/$ - see front matter © 2012 Elsevier B.V. All rights reserved.
http://dx.doi.org/10.1016/j.chemphys.2012.08.010

films will thus help in finding the nature of the Cl-passivated Ge surface and in addition it will be act as a passivation layer [17].

In this article, using X-ray photoelectron spectroscopy (XPS), CA measurement, X-ray reflectivity (XRR) and atomic force microscopy (AFM) techniques we have investigated the wettability of the Cl-passivated Ge surface. Our analysis suggests that although the surface shows an intermediate wettability behavior but the surface is effectively homogeneous and hydrophilic (~85%) along with very few hydrophobic (~15%) regions. The electrostatic and dispersive contributions of Cl atoms are possibly responsible for such surface nature.

## 2. Experimental

Ge(001) substrates were cut into pieces (of size 20 mm × 10 mm) and were sonicated, first in the presence of trichloroethylene (for about 10 min) and followed by methyl alcohol (for ~10 min), to remove organic contaminants. Then the substrates were dipped into dilute (10%) HCl solution for 10 min in order to do the chlorination of the Ge(001) substrates and resulting substrates were labeled as Cl–Ge. NiA LB films were deposited by one (up) and two (down-up) strokes on Cl–Ge surfaces and were referred as 1s-NiA/Cl–Ge and 2s-NiA/Cl–Ge, respectively.

Arachidic acid [$CH_3(CH_2)_{18}COOH$, Sigma, 99%] molecules were spread from a 0.5 mg/ml chloroform (Aldrich, 99%) solution on Milli-Q water (resistivity 18.2 MΩ cm) containing nickel sulphate ($NiSO_4{\cdot}2H_2O$, Merck, 99%) in a Langmuir trough (Apex Instruments). The pH of the water subphase containing 0.2 mM nickel sulphate was maintained at 8.5–9.0 using sodium hydroxide (NaOH, Merck, 98%). No buffers were used to maintain the pH of the subphase. Nearly 8 h were spent for pH stabilization including initial magnetic stirring. Prior to deposition, surface pressure-specific molecular area ($\pi - A$) isotherm of NiA Langmuir monolayer on water surface was recorded. $\pi$ was measured with a Wilhelmy plate and the monolayer was compressed at a constant rate of 3 mm/min. All depositions were done at $\pi$ = 30 mN/m and at room temperature (22 °C). Depositions were carried out at a speed of 2 mm/min.

Cl-passivation of the Ge surfaces was verified by XPS measurements. XPS measurements were performed at base system pressure of $1 \times 10^{-9}$ mbar in a multiprobe chamber (Omicron NanoTechnology) equipped with an Al $K\alpha$ (1486.6 eV) source and a hemispherical analyzer (EA 125).

CA measurements were carried out using home built setup to verify the hydrophilic or hydrophobic nature of the Ge(001) substrate before and after the chlorination. A drop (4 µl) of Milli-Q water was placed on the sample surface using a micro syringe. The image of water droplet on the substrate surface was captured by a traveling microscope followed by a digital camera. The images were analyzed using IMAGEJ software. The experiment was repeated at different regions over the sample surface.

XRR measurements were carried out using a versatile X-ray diffractometer (VXRD) setup to investigate the structure of NiA LB films deposited on Cl–Ge(001) substrates. VXRD consists of a diffractometer (D8 Discover, Bruker AXS) with Cu source (sealed tube) followed by a Göbel mirror to select and enhance Cu $K\alpha$ radiation ($\lambda$ = 1.54 Å). The diffractometer has a two-circle goniometer ($\theta$–2$\theta$) with quarter-circle Eulerian cradle as sample stage. The latter has two circular ($\chi$ and $\varphi$) and three translational (X, Y, and Z) motions. Scattered beam was detected using NaI scintillation (point) detector. Data were taken in specular condition, i.e., the incident angle ($\theta$) is equal to the reflected angle ($\theta$) and both are in a scattering plane. Under such condition, a non-vanishing wave vector component, $q_z$, is given by $(4\pi/\lambda)\sin\theta$ with resolution 0.0014 Å$^{-1}$. XRR technique essentially provides an electron density profile (EDP), i.e., in-plane ($x - y$) average electron density ($\rho$) as a function of depth ($z$) in high resolution [9,10]. From EDP it is possible to estimate film thickness, electron density, and interfacial roughness. Analysis of XRR data was carried out using Parratt's formalism [26]. For the analysis, the films were divided into a number of layers including roughness at each interface.

The topography of the LB films on the Cl–Ge substrate was mapped through AFM technique (Beam-deflection AFM, Omicron NanoTechnology) in different length scales and in different portions of the samples, after completion of XRR measurements. AFM images were collected in noncontact mode using silicon cantilever (dimensions ≈ 125 µm × 30 µm, spring constant ≈ 42 N/m, resonance frequency ≈ 320 kHz) and sharp niddle like tip and in UHV (~$10^{-9}$ mbar) conditions to minimize the tip induce modification of the LB films and to get clean images, respectively. WSxM software [27] was used for image processing and analysis.

## 3. Results and discussion

### 3.1. X-ray photoelectron spectroscopy study

The Cl 2p and Ge $2p_{3/2}$ core-level spectra of the Cl–Ge sample are shown in Fig. 1a and b. All the XPS data were taken just after the surface chlorination. The two peaks (indicated by dash and dash-dot lines) shown in Fig. 1a, at ≈ 200 eV and ≈ 201.8 eV represent the two Cl 2p spin–orbit split peaks i.e., $p_{3/2}$ and $p_{1/2}$ respectively. The broad peak positioned at ≈ 200.3 eV, shown by dash-dot line, is attributed to the Ge 3s plasmon loss peak. The solid line, which is the fit of the raw data, is the sum of the $p_{3/2}$ and $p_{1/2}$ peaks of Cl 2p. The Ge $2p_{3/2}$ spectrum (shown in Fig. 1b) is clearly seen to have two components. The slightly higher intense component at ≈ 1218 eV (indicated by dashed line) is coming from the bulk Ge $2p_{3/2}$ contribution. The second component (indicated by dashed line) at ≈ 1219.7 eV with a chemical shift of 1.7 eV with respect to the previous one, is attributed to the surface Ge atoms, which are bonded to the more electronegative Cl atoms [5]. This

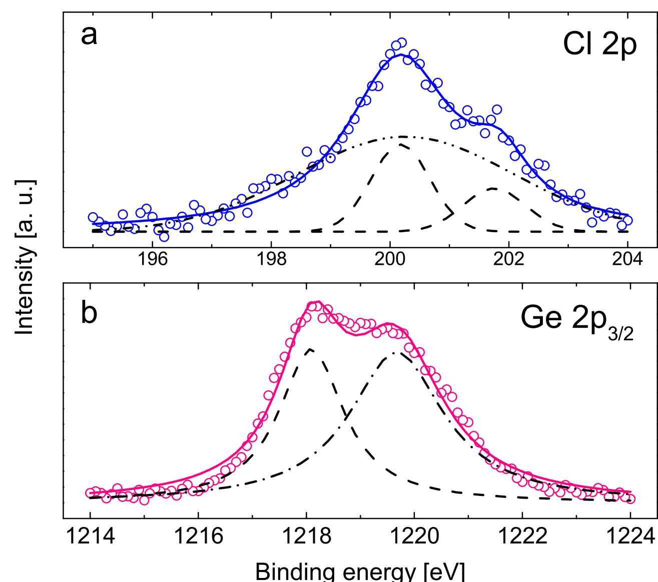


**Fig. 1.** XPS spectra taken on Cl–Ge surface: (a) The Cl 2p core-level spectrum. The open circles are experimental data. The dashed lines are two components of Cl $2p_{3/2}$, $2p_{1/2}$ spin–orbit doublet. The dotted line is from Ge 3s plasmon loss. (b) The Ge $2p_{3/2}$ core-level spectrum. The open circles are experimental data. The dashed line and the dash-dot line represent the contribution from bulk Ge(–Ge) and surface Ge(–Cl), respectively. In both cases, the solid line represents the sum of their corresponding two components.

peak may represent a convolution of multiple peaks originated by Ge–Cl, H–Ge–Cl and $H_2$–Ge–Cl bonding. Although the formation of Ge–Cl bond is energetically favored that will be discussed later in detail.

### 3.2. Contact angle measurements

The wettability of the Ge substrate after ultrasonic cleaning and after Cl-passivation (i.e., Cl–Ge) was investigated by CA measurements. The CA of water on the ultrasonic cleaned Ge surface is ~51° and on the Cl–Ge surface is ~39°. It suggests that due to the immersion of Ge substrate into HCl solution, i.e., after the Cl-passivation the surface wettability is increased. The $\theta$ value of Cl–Ge surface implies that the resulting surface cannot be called as completely hydrophilic or hydrophobic surface, rather it will be more appropriate to called it as a "hydrophilic-like" surface.

### 3.3. Structural study of LB films grown on Cl–Ge surface

LB films are usually made by amphiphilic molecules where hydrophilic 'head' and hydrophobic 'tail' parts are present [28,29]. Depending upon the nature of the substrate surface such molecules after deposition, i.e., in LB film, take the favorable structure. On the hydrophilic substrate, molecules attach the substrate surface through the hydrophilic 'head' and the hydrocarbon 'tails' remain towards the air to form asymmetric molecular layer (AML) or conventional monolayer in one (up) stroke, while on the hydrophobic substrate, molecules attach the substrate surface through the hydrophobic 'tail' and they remain both sides of the 'head' to form symmetric molecular layer (SML) or conventional bilayer structure in two strokes (down-up) [24]. As the XRR technique provides EDP along depth in Å level, it is possible to find out the structures (AML or SML) of the NiA molecules in the LB films. By knowing these out-of-plane structures, the hydrophilic/hydrophobic nature of the Cl–Ge substrate surface can be obtained as the specific structure formation is strongly related with the hydrophilicity/hydrophobicity of the substrate [24,25]. Though LB transfer is complex as it depends on various factors like, pH of subphase water, deposition pressure, monolayer compression rate, etc. however, a suitable choice of those parameters can bypass the complexity. In our study, we have standardized those parameters to get a good LB film on a particular substrate and indeed, we have become successful in achieving very good films on substrates [24,25]. A particular choice of the above mentioned parameters enable us to form LB films on completely hydrophilic, completely hydrophobic and coexisting surfaces. Moreover, we did not observe any appreciable defects other than the "pinhole" type defects, which are the characteristics of LB film. In our previous works [24,25], we have successfully shown that the LB structure on a substrate surface is exactly following the hydrophobic and hydrophilic nature of the surface. For homogeneous natured surface (H- and OH-passivated Si surface) a perfect LB film with suitable structure was formed but for inhomogeneous surface (Br-passivated Si surface), where hydrophobic and hydrophilic domains coexist, an imperfect LB film was formed. From these consequences, it can be conclude that the idea about the homogeneity or inhomogeneity of a surface can be predicted from the nature of the LB film growth and the deposited film structure.

The XRR profiles of 1s-NiA/Cl–Ge and 2s-NiA/Cl–Ge samples (shown in Fig. 2) show a significant difference in the oscillations which are more distinct in latter case. It implies that the interfaces of different layers in 1s-NiA/Cl–Ge sample are rougher than that of 2s-NiA/Cl–Ge sample. A low density layer above $z = 3$ nm is clearly seen in the EDP (inset of Fig. 2) of 2s-NiA/Cl–Ge sample unlike to the 1s-NiA/Cl–Ge sample. It suggests that for both the samples, surfaces are effectively covered by the AML structure of NiA molecules although few SML molecules are observed only in the 2s-NiA/Cl–Ge sample (shown by cartoon pictures in the EDP). From the EDP we have roughly quantified the coverage of individual structures considering the maximum tail density 0.33 e/Å$^3$ as 100% coverage. The $\rho$ value of the top tail part of 2s-NiA/Cl–Ge sample, which is nothing but the SML structural contribution, is 0.05 e/Å$^3$. Thus, the coverage of SML structure is ~15%. As the overall LB film is compact, the rest of the ~85% area is covered by AML. Higher roughness and less upright length of SML structures (~15%) in 2s-NiA/Cl–Ge sample indicate the randomly tilted organization of molecules. The EDP of 2s-NiA/Cl–Ge sample (shown in Fig. 2) suggests the AML structures (~85%) are untilted. The reason for which the SML molecules are tilted and the others i.e., AML molecules remain untilted can be explained as follows. The Cl-passivated Ge surface is not completely hydrophilic rather it is more likely to be hydrophilic-like as observed from the CA. Thus it is highly possible to attach of the tail part of the molecules with the weakly hydrophilic surface at the time of down stroke in order to form SML structure on the surface. Some of SML molecules may form due to the presence of the hydrocarbon contaminations on the substrate surface. At the time of down stroke ~15% area is covered by the SML structure but rest of area i.e., ~85% area remains vacant which is filled by the AML molecules in the up stroke. Those SML molecules are tilted whereas the AML molecules remain untilted. The SML molecules that are attached therefore have an excess surface area and can easily tilt [30]. In the up stroke the AML molecules that attached in the remaining vacant area, do not have much freedom, which essentially force them to remain untilted. Thus, the initial attachment of the molecules with the substrate is controlling the growth or arrangement of the rest of the film.

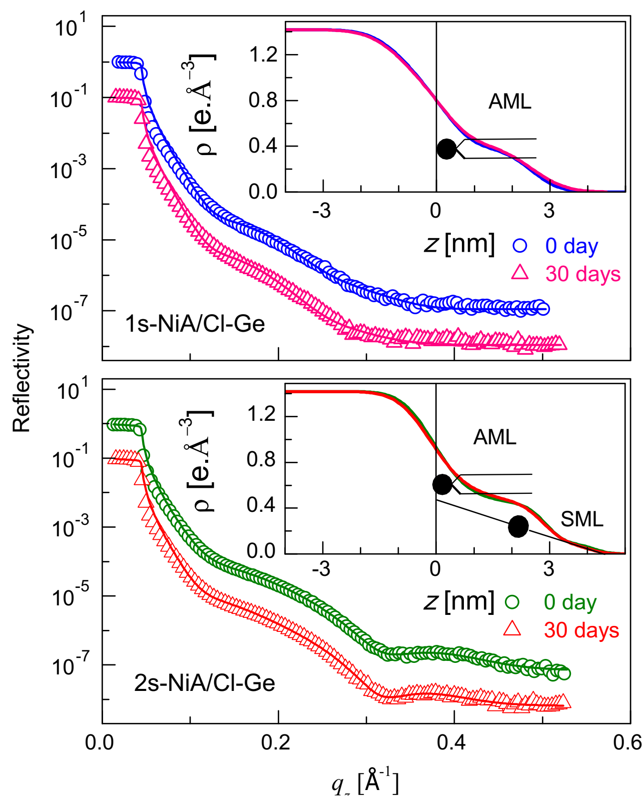


**Fig. 2.** XRR data (open circles) and analyzed curves (solid line) of 1s-NiA/Cl–Ge (upper panel) and 2s-NiA/Cl–Ge (lower panel) LB films. Insets: Corresponding EDPs and cartoons of film structures.

AFM images of 1s-NiA/Cl–Ge and 2s-NiA/Cl–Ge samples are shown in Fig. 3a and b respectively. Topography of 1s-NiA/Cl–Ge

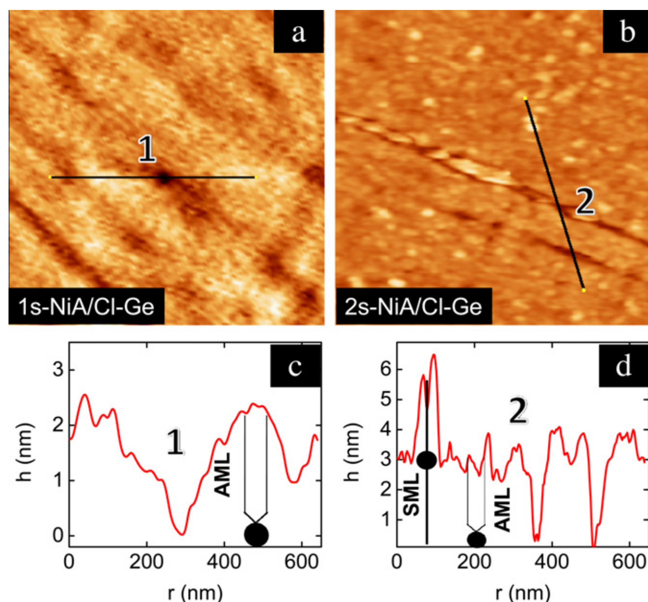


**Fig. 3.** AFM images in length scale 1000 × 1000 $nm^2$ of (a) 1s-NiA/Cl–Ge and (b) 2s-NiA/Cl–Ge samples. (c and d) Represent height profiles of the drawn lines 1 and 2 respectively along with the AML and SML cartoons.

sample is similar to that of a standard homogeneous NiA monolayer (AML) LB film, which is obtained from the AFM line profile and is supported from the EDP (shown in Fig. 2). However, in 2s-NiA/Cl–Ge sample, apart from the single height (≈ 3 nm), i.e., of AML structure, few large height (≈ 6 nm) islands, which corresponds to SML structure, are present. Typical line profiles shown in Fig. 3c and d represents the film heights. The presence of such islands of SML structure in 2s-NiA/Cl–Ge sample is also identified from XRR analysis. From the AFM image (shown in Fig. 3a) analysis we have calculated the SML coverage by selecting only those hills whose heights are greater than the AML height i.e., ≈ 3 nm. The coverage obtained is similar to that of obtained from the EDP. In 1s-NiA/Cl–Ge sample, SML could not formed and those regions remain vacant which is evident from few small sized holes of depth <2.5 nm, one of them is shown in the AFM topography (Fig. 3a and c). Moreover, the molecules of AML structure will be tilted towards the adjacent uncovered hydrophobic regions, which results in more roughened AML structure compared to that of 2s-NiA/Cl–Si. Accordingly the film-substrate interfacial roughness, which is calculated from the EDPs (shown in Fig. 2), is greater for 1s-NiA/Cl–Si sample (≈ 11 Å) than that for 2s-NiA/Cl–Si sample (≈ 8 Å).

In our previous study [24], we have shown that SML structure can form not only in two strokes but also in single up stroke if there are relatively strong hydrophobic regions within hydrophilic surface. Here, we observed that the SML structure is only formed in two strokes. This indicates that the hydrophobicity is not so strong. Thus, the structures of the LB films signify the uniform hydrophilic-like nature of the Cl–Ge surface. XRR data from both the samples also were taken nearly after 30 days and no appreciable change were observed in reflectivity profiles and hence in EDPs. It reflects the good stability of the LB films on Cl–Ge surface.

### 3.4. Nature of Cl-passivated Ge surface

From XPS study, it is clear that the Ge surface is well passivated by Cl. In HCl treatment, initially oxide is removed by Cl atoms and the resulting surface is terminated by Cl. The passivation reaction ends here, which is unlike to the H-passivation by HF treatment [21]. In HF treatment, the surface is first terminated with F upon removal of native oxide layer. However, the eletronegativity difference between Ge–F (1.97) is greater than the Ge–Cl (1.16). Furthermore, compared with the Ge–F bonds (bond strength ≈ 470 kJ/mol, bond length ≈ 168 pm), Ge–Cl bonds (bond strength ≈ 349 kJ/mole, bond length ≈ 210 pm) have a weaker bond strength and a longer bond length. As a result, Ge–F bonds become more polarized than Ge–Cl bonds and hence the Ge–F bonds will be further attacked by the HF in order to form mostly H-passivated surface although some of the bonds are still terminated by F atoms. Whereas, Ge–Cl bonds become resistant to further attacking of HCl, which helps the Cl atoms to remain on the Ge surface by terminating the dangling bonds. It suggests the possibility of homogeneous and stable passivation of Ge surface by a single chemical species Cl.

CA measurements show the intermediate wetting behavior of Cl–Ge surface. However, from structural study we observed that such intermediate wetting behavior of Cl–Ge surface is not coming due to the coexistence of hydrophobic and hydrophilic domains. Intermediate wetting behavior or intermediate CA can form on surfaces for two different situations, which are shown schematically in Fig. 4. The first situation arises when the surface is inhomogeneous, i.e., strong hydrophilic and strong hydrophobic domains, whose size $A_D$ < size of water droplet $A_W$, coexist [23] and the

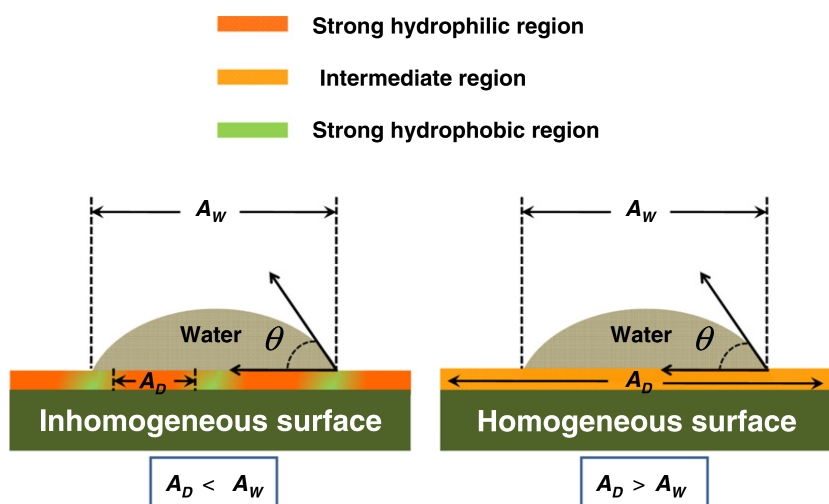


**Fig. 4.** Side view of a sessile liquid drop on inhomogeneous and homogeneous surfaces. θ is the contact angle of a liquid drop on such surfaces.

second situation arises when the surface is homogeneous ($A_D > A_W$) but the intensity of hydrophilicity or hydrophobicity is less. The former case i.e., coexistence of hydrophobic and hydrophilic domains (size ~ few nanometer) was observed for Br-passivated Si surface [24] and also for H-passivated Si surface after immersed into high pH subphase water [25]. The nature of such domains, whose size $A_D < A_W$, was extracted by studying the growth of the NiA LB film as the growth occurs molecule-by-molecule. In Br-passivated Si surface, the surface is fractionally terminated by Br-atoms, which is hydrophobic in nature and the rest of the portion is covered by native oxide, which is hydrophilic in nature [24]. Hence, the CA of water on Br-passivated Si surface becomes ~55°. In case of H-passivated surface, which is originally hydrophobic, strong hydrophilic regions (OH-terminated regions) are incorporated by immersion into high pH water. As a result H-passivated Si surface after immersion into high pH water shows mixed behavior i.e., some portions are strongly hydrophobic and some portion becomes strongly hydrophilic [25]. The CA of water on such surface becomes ~34°. Thus, intermediate wettability indicates the coexistence of hydrophilic and hydrophobic domains of such passivated Si surfaces. However, the details about the coverages of hydrophilic and hydrophobic domains are obtained from the structural study after depositing the NiA LB films on such surfaces. The coverages of AML and SML structures, which usually form on hydrophilic and hydrophobic surfaces, give the corresponding domain coverages. Thus, Br-terminated Si has ~60% hydrophilic and ~40% hydrophobic domains, whereas H-passivated Si surface after immersed into high pH subphase water has ~80% hydrophilic and ~20% hydrophobic domains.

It should be mention here that in LB deposition, single up stroke is generally used for the deposition on hydrophilic substrate surface whereas two strokes i.e., down-up sequence is used for the deposition on hydrophobic surface. At the time of upstroke, subphase water wets the hydrophilic substrate and hence amphiphilic molecules are attached with the substrate surface through the head by head-substrate hydrophilic interaction ($E_{\text{head-sub}}$) in order to form AML structure. This $E_{\text{head-sub}}$ is relatively stronger than the head-subphase water hydrophilic interaction ($E_{\text{head-water}}$), which tries to keep the amphiphilic molecules on the water surface. It is also possible to form SML structure in coexistence with the AML, in single up stroke, provided strong hydrophobic domains are present along with the hydrophilic domains that we have observed previously in case of Br-passivated Si and for H-passivated Si dipped in water subphase of elevated pH [24,25]. On the other hand, in down-up cycle, at the time of down stroke effective transfer of amphiphilic molecules depends upon the competition between $E_{\text{head-water}}$ and $E_{\text{tail-sub}}$, where the later is the tail-substrate hydrophobic interaction which tries to transfer the molecules from water to substrate surface. If $E_{\text{head-water}} > E_{\text{tail-sub}}$, then ideally no transfer of molecules occurs, which happens for hydrophilic surfaces. Whereas, if $E_{\text{head-water}} < E_{\text{tail-sub}}$, transfer will take place and the molecules will be attached with the substrate through tails to form SML structure. This situation is generally observed for hydrophobic surfaces. Presence of only AML structure in 1s-NiA/Cl–Ge sample suggests that the Cl–Ge surface is hydrophilic and strong hydrophobic domains of appreciable size are absent. Whereas in 2s-NiA/Cl–Ge sample, very small amount (~15%) of SML structure along with mostly (~85%) AML structure again verifies that Cl–Ge surface has a hydrophilic-like tendency. Absence of native oxide and presence of mostly AML structure suggests that the Cl–Ge surface is effectively homogeneous, i.e., covered by only one type of domain which is hydrophilic, although very less (~15%) hydrophobic regions are present. The information obtained from the CA measurements and LB film growth suggests that although the surface is homogeneous hydrophilic but this hydrophilicity is intermediate, or more precisely relatively weak.

The weak hydrophilicity of Cl–Ge surface can be attributed to the nature of the Cl atoms placed on the Ge matrix. Owing to lower electronegativity of Cl atoms (~3.16 in Pauling scale) in comparison with O atoms (~3.44), it has a less affinity to the water molecules and as a result, the Cl-passivated surface is expected to behave as a less hydrophilic surface. The electronegativity difference between Cl and Ge is not so high and accordingly it assesses the formation of weak H-bond between the Cl atoms and the polar molecules (i.e., water, head part of amphiphilic molecules). Apart from that, there are another two interactions namely, electrostatic and dispersive interactions, which are also to some extent, establish the hydrophobic or hydrophilic character of the substrate surface [19]. In case of Cl, these two interactions are likely to be strong due to the presence of large number of electrons, which may be responsible for the hydrophilic-like character of Cl–Ge surface. On the other hand, the electronegativity of Cl is more than Br (~2.96). Br–Si surface shows towards hydrophobic character [24] as Br could not form the H-bond with the polar molecules due to the relatively small electronegativity difference between Br and Si atoms. Probably a fine-tuning of the electronegativity value of the passivated atoms is responsible for the hydrophilic or hydrophobic nature of the substrate surface. Moreover, no appreciable change in the structure of the NiA LB film grown on Cl–Ge surface is observed with time (shown in Fig. 2) indicating quite stable interface, which perhaps due to unpolarized and strong bond strength effect of Ge–Cl bonds. Furthermore, owing to have the large atomic size the Cl atoms (covalent radii ≈ 0.99 Å) and hence the Cl-passivating layer may provide a strong steric barrier for the oxygen molecules in reaching the underlying Ge(001) surface [31]. Perhaps such properties are responsible for the better stability of the homogeneously passivated Cl–Ge surface. Although the long-term exposure of the bare Cl–Ge surface under ambient condition may slightly oxidize the surface due to the reaction with ambient oxygen and water molecules. The presence of the overlayer compact NiA LB film may inhibit the oxidation by blocking the open access of oxygen to the Cl–Ge surface which further improves the stability of the Cl–Ge surface. It offers the possibility of using these passivated semiconductor surfaces in the fabrication of organic devices for some novel applications.

## 4. Conclusion

We have performed XPS, CA and LB film growth studies to investigate the wettability of Cl-passivated Ge(001) surface. XPS results confirm the well passivation of Ge surface by Cl atoms. CA measurements indicate the intermediate wettability of that surface, whereas structural study of the LB films deposited in one stroke (~100% AML) and in two strokes (~85% AML and ~15% SML) show that the Cl–Ge surface is effectively homogeneous and hydrophilic-like in nature. Such intermediate or hydrophilic-like behavior possibly comes due to the presence of specific electrostatic and dispersive contributions of Cl atoms. Moreover, stability of the LB films on such Cl–Ge substrate implies that such passivated substrate will be useful for the fabrication of organic devices for future applications.

## Acknowledgements

Authors acknowledge Prof. A.K. Raychaudhuri of S.N. Bose National Centre for Basic Sciences, Kolkata for his support to access LB trough facility. The authors thank Mr. A.K.M. Maidul Islam and Prof. M. Mukherjee of Surface Physics Division, Saha Institute of Nuclear Physics for their help in XPS measurements and Prof. S. Banerjee and Ms. A. Bhattacharya of Surface Physics Division, Saha Institute of Nuclear Physics for their help in contact angle

measurements. S. Kundu acknowledges the financial support from Department of Science and Technology.

## References


[1] J. Travis, Science 262 (1993) 1819.
[2] R. Driad, Z.H. Lu, S. Charbonneau, W.R. McKinnon, S. Laframboise, P.J. Poole, S.P. McAlister, Appl. Phys. Lett. 73 (1998) 665.
[3] G.W. Anderson, M.C. Hanf, P.R. Norton, Phys. Rev. Lett. 74 (1995) 2764.
[4] X.G. Zhang, Electrochemistry of Silicon and its Oxide, Kluwer Academic, New York, 2004.
[5] Z.H. Lu, Appl. Phys. Lett. 68 (1996) 520.
[6] H. Ubara, T. Imura, A. Hiraki, Solid State Commun. 50 (1984) 673.
[7] E. Yablonovitch, D.L. Allara, C.C. Chang, T. Gmitter, T.B. Bright, Phys. Rev. Lett. 57 (1986) 249.
[8] V.A. Burrows, Y.J. Chabal, G.S. Higashi, K. Raghavachari, S.B. Christman, Appl. Phys. Lett. 53 (1988) 998.
[9] J.K. Bal, S. Hazra, Phys. Rev. B 75 (2007) 205411.
[10] J.K. Bal, S. Hazra, Phys. Rev. B 79 (2009) 155412.
[11] W. Kern, D.A. Puotinen, RCA Rev. 31 (1970) 187.
[12] N. Hirashita, M. Kinoshita, I. Aikawa, T. Ajioka, Appl. Phys. Lett. 56 (1990) 451.
[13] G.S. Higashi, Y.J. Chabal, G.W. Trucks, K. Raghavachari, Appl. Phys. Lett. 56 (1990) 656.
[14] H.F. Okorn-Schmidt, IBM J. Res. Dev. 43 (1999) 351.
[15] G.W. Trucks, K. Raghavachari, G.S. Higashi, Y.J. Chabal, Phys. Rev. Lett. 65 (1990) 504.
[16] K. Sekar, P.V. Satyam, G. Kuri, D.P. Mahapatra, B.N. Dev, Nucl. Instrum. Methods Phys. Res. B 71 (1992) 308.
[17] J. Terry, R. Mo, C. Wigren, R. Cao, G. Mount, P. Pianetta, M.R. Linford, C.E.D. Chidsey, Nucl. Instrum. Methods Phys. Res. B 133 (1992) 94.
[18] C.-Y. Ruan, V.A. Lobastov, F. Vigliotti, S. Chen, A.H. Zewail, Science 304 (2004) 80.
[19] P.L. Silvestrelli, F. Toigo, F. Ancilotto, J. Phys. Chem. B 110 (2006) 12022.
[20] C.H. Lee, Z.D. Lin, N.G. Shang, L.S. Liao, I. Bello, N. Wang, S.T. Lee, Phys. Rev. B 62 (2000) 17134.
[21] S. Sun, Y. Sun, Z. Liu, Dong-Ick Lee, S. Peterson, P. Pianetta, Appl. Phys. Lett. 88 (2006) 021903.
[22] G. Kissinger, W. Kissinger, Phys. Stat. Sol. A 123 (1991) 185.
[23] S. Adachi, T. Arai, K. Kobayashi, J. Appl. Phys. 80 (1996) 5422.
[24] J.K. Bal, S. Kundu, S. Hazra, Phys. Rev. B 81 (2010) 045404.
[25] J.K. Bal, S. Kundu, S. Hazra, Chem. Phys. Lett. 500 (2010) 90.
[26] L.G. Parratt, Phys. Rev. 95 (1954) 359.
[27] I. Horcas, R. Fernndez, J.M. Gwez-Rodrguez, J. Colchero, J. Gomez-Herrero, A.M. Baro, Rev. Sci. Instrum. 78 (2007) 013705.
[28] K.B. Blodgett, I. Langmuir, Phys. Rev. 51 (1937) 964.
[29] M.C. Petty, Langmuir–Blodgett Films, an Introduction, Cambridge University Press, New York, 1996.
[30] S. Hazra, A. Gibaud, A. Desert, V. Gacem, N. Cowlam, Physica B 283 (2000) 45.
[31] S. Sun, Y. Sun, Z. Liu, D.-I. Lee, P. Pianetta, Appl. Phys. Lett. 89 (2006) 231925.